Int J Adv Manuf Technol (2017) 91:2787–2797
DOI 10.1007/s00170-016-9922-4

ORIGINAL ARTICLE

A study on the tool edge geometry effect on nano-cutting

Feifei Xu[1,2] · **Jinshi Wang**[1] · **Fengzhou Fang**[1] · **Xiaodong Zhang**[1]

Received: 15 July 2016 / Accepted: 18 December 2016 / Published online: 11 January 2017

Abstract The tool edge has a significant influence on a cutting process especially when it is comparable to uncut chip thickness. Generally, the cutting tool edge is considered rounded and is characterized by a tool edge radius. When the cutting tool edge geometry is not a symmetrical circle, the tool edge radius fitted with the former methods is not sufficient to describe the performance of the cutting edge. In this study, a parameter, which is different from the previous description method, is proposed to characterize the tool edge. Three different tool edges are reconstructed to investigate the effect of the proposed parameter on a nano-cutting process using molecular dynamics. Results show that combined with the former used tool edge radius, the newly proposed tool edge characterization parameter which is the tool edge radius fitted with the edge profile at the flank face side could be used to characterize the cutting performance of an asymmetric tool edge. The minimum uncut chip thickness, subsurface damage, and cutting force in feed direction investigated in this study tend to increase with the newly proposed characterization parameter. A stagnation region formed in front of the cutting edge acts as a new formed cutting edge making the material removed in shearing mechanism when the uncut chip thickness is larger than the minimum uncut chip thickness. However, when it is similar or smaller than minimum uncut chip thickness, the stagnation region is not tough enough to cut the materials making it to slide on the surface and part of the atoms in the upper layer of workpiece is removed by extrusion. Two models are proposed to describe the shearing and extrusion mechanism in a nano-cutting process.

Keywords Nano-cutting · Tool edge geometry · Stagnation region · Surface integrity

✉ Fengzhou Fang
fzfang@tju.edu.cn

[1] State Key Laboratory of Precision Measuring Technology & Instruments, Centre of MicroNano Manufacturing Technology, Tianjin University, Tianjin 300072, China

[2] Institute of Mechanical Manufacturing Technology, China Academy of Engineering Physics, Sichuan 621900, China

1 Introduction

The tool edge which was usually neglected in conventional machining processes, such as the shear plane model proposed by Merchant [1, 2], has become important parameters in influencing the process of micro- and nano-cutting [3–6], such as the chip formation [7], surface generation [8], and minimum uncut chip thickness [9]. The form of the cutting edge is defined in micro-geometry as the transition between the rake face and the flank face of a cutting wedge [10]. The form of the tool edge is simply considered rounded and is characterized by an edge radius r_w. The effect of a tool edge radius was studied by Chien [11] and Albrecht [12]. After that, many studies have been conducted to investigate the influence of the tool edge on the cutting process. Such the hydrostatic pressure under the tool edge is beneficial to cut brittle materials in a ductile region studied by Fang et al. in 1998 [13]. When the tool edge cannot be ignored, there is a threshold below which the chip formation cannot be formed stably or even no chip formation. Kim et al. [14] observed ploughing under a certain uncut chip thickness (UCT) which indicates the existence of a threshold. The threshold is defined by Ikawa et al. as the minimum UCT that can be removed stably from a workpiece surface with a cutting edge under perfect performance [15]. The minimum UCT determines the extreme accuracy attainable under specific cutting conditions, tool and workpiece, etc.

The minimum UCT strongly relates to the material separation mechanisms in front of the tool edge. Two major approaches have been proposed to analyze the material separation mechanism [10, 16]. The first approach is based on the existence of a stagnation point on the tool round edge, below which the material flow under the tool to form the machined surface and above which the material flow up along the tool face to form a chip [17]. The second approach is based on the existence of a stagnation region in front of the tool edge like a stable build-up edge (BUE) or a dead metal zone (DMZ) which changes the flow of workpiece material. The tip of a stagnation zone is where the workpiece material starts to split into two parts. The formation of a stagnation zone or dead metal zone is determined by the tool edge shape, cutting speed, material and frictional properties of the tool, and workpiece materials [18].

However, the characterization of the tool edge is almost depending on individual researchers, measurement uncertainty, and fitting algorithm. These factors would cause discrepancies in describing the tool edge with the tool edge radius [19]. Therefore, a common understanding for the influence of the tool edge on a cutting process is inhibited by the poor detected consistency. Wyen et al. proposed a new algorithm to increase the repeatability in characterizing the cutting edge radius by making the choice of fitting area user independent [20]. For the cutting edge which is not a symmetrical circle, they also developed a method in characterizing the asymmetry of cutting edges [21]. Yussefian et al. [22] proposed a method to identify the cutting edge by adapting placement of the knots that minimizes the residual error from fitting the B-spline to the tool profile data. Subsequently, the edge is modelled by parametric quadratics. Four parameters are derived to characterize the cutting edge which is symmetric or asymmetric. Denkena et al. proposed the form factor method (also referred to as K-factor method) to characterize the shape of a tool edge, especially when the cutting edge is asymmetrical [23]. Four parameters S_α, S_γ, Δr, φ are introduced, and the average cutting edge rounding $\overline{S}$ and the form factor K (Kappa) were deduced to respectively specify the dimension and shape of the rounding at the cutting edge. The influences of the S_α, S_γ on the cutting force are investigated, and results show that the process forces are mostly affected by the edge segment on the flank face, S_α, whereas the impact of the segment on the rake face, S_γ, is negligible.

In a nano-cutting process, cutting tools are usually used to generate parts with nano-metric surface finish. The feature size of the tool edge can achieve 10 to 100 nm which is smaller than those of the tungsten carbide or PCBN inserts [24, 25]. Therefore, how to measure the shape of a tool edge accurately and to analyze the effect of the tool edge shape on a micro-/nano-cutting process becomes a significant issue. Atomic force microscopy (AFM) is an effective method in measuring the shape of a tool edge for its nano-metric vertical and lateral resolution. The copied profile of a cutting tool edge which is formed by indenting the cutting edge into the surface of copper has been measured by AFM [26]. However, when the tool edge is directly measured by AFM, it is difficult to align AFM tip with the tool edge due to the low depth-of-field and poor resolution of the optical microscope in conventional AFM. Gao et al. [27, 28] combined an AFM with an optical sensor for alignment of the AFM probe tip with the tool edge in a sub-micrometer range more easily.

In practice, the evaluation of the nano-metric tool edge radius has the same problem mentioned by Bassett et al. which is the measurement inaccuracy caused by different operators and algorithms [29]. Therefore, a measurement standard for a tool edge needs to be established, and relationship between tool edge shape and a cutting process should be investigated and understood by the researchers to choose and fabricate a perfect tool for different applications. However, the former proposed characterization parameters are too complicated to apply in the industry. Hence, in this paper, a simple characterization parameter is proposed and the influences of the asymmetrical tool edge on the nano-cutting process are discussed.

2 Reconstruction and characterization of tool edges

2.1 Reconstruction of a tool edge

The shape of the tool edge is always characterized by an edge radius r_β. However, the real shape of the tool edge is deviated from the ideal edge radius, and the characterization methods have been proposed by Denkena et al. [23] and Wyen et al. [21]. For simulating the influences of the deviation on a cutting process, the tool edge is reconstructed by the parameters proposed by Denkena et al. [23], as shown in Fig. 1. In this study, the difference from the previous method is that the vector Δr is perpendicular to the profile of the tool edge and intersects at point B. It could also be seen as a tangent circle with a radius of Δr and center locating at point E which is the intersection point of the extended lines of flank face and rake fake. The direction of the vector Δr is characterized by the angle φ which is the included angle between the vector Δr and bisector of the tool edge. The separation points of the cutting edge rounding at flank face and rake face are points A and C, and the length of the extended line are S_α and S_γ. Parameter r_s is the basic circle radius to constrain the size of the reconstructed tool edge. If the form factor $K = S_\gamma / S_\alpha = 1$, the radius could be determined by the equation:

$$r_s = S_a \cdot \tan\theta \tag{1}$$

$$\theta = \frac{\pi}{4} - \frac{\alpha}{2} - \frac{\gamma}{2} \tag{2}$$

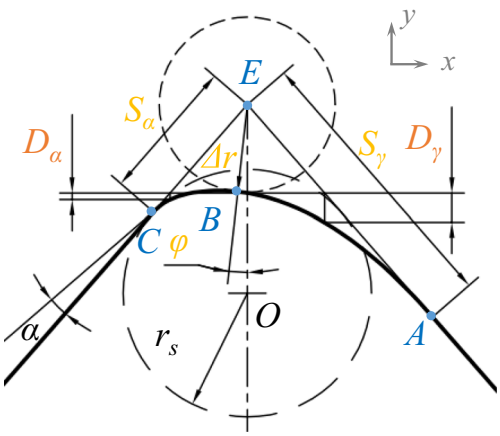

Fig. 1 Characterization of cutting tool edge shape

where α is the flank angle, γ is the rake angle. D_α and D_γ in Fig. 1 are the parameters proposed by Wyen et al. [21] to determine the asymmetry of the tool edge by D_γ/D_α. Therefore, the position of three points A, B, and C and their derivative could be determined by the parameters mentioned above. Hermite interpolation is applied to reconstruct the tool edge by the point:

$$A : (x, y, y') = \left(S_\gamma \cdot \sin\theta, r_s \Big/ \sin\theta - S_\gamma \cdot \cos\theta, -\cot\theta\right) \quad (3)$$

$$B : (x, y, y') = \left(\Delta r \cdot \sin\varphi, r_s \Big/ \sin\theta - \Delta r \cdot \cos\varphi, \tan\varphi\right) \quad (4)$$

$$C : (x, y, y') = \left(-S_\alpha \cdot \sin\theta, r_s \Big/ \sin\theta - S_\alpha \cdot \cos\theta, \cot\theta\right) \quad (5)$$

The position of the points is deduced based on the coordinate original point locating at the center of a basic circle. If the vector Δr rotates clockwise, the angle $\varphi < 0$, else $\varphi > 0$.

Three tool edges are reconstructed by sets of parameters listed in Table 1. The nominal rake angle and clearance angle of three tool edges are respectively 0° and 8°. The form factors K of tool edges T1, T2, and T3 are 2, 1, and 0.5. The shape of the tool edges is shown in Fig. 2. A molecular dynamic (MD) study is applied in modelling nano-metric cutting of single-crystal silicon. The cutting tool was assumed to be perfectly rigid. The workpiece has a size of 20 nm × 40 nm (height × length), including more than 25,000 silicon atoms, and defined as three kinds: boundary atoms, thermostat atoms, and Newtonian atoms. Periodic boundary condition is applied along the z direction in the model. The UCT of nano-metric cutting is 5 nm. The Tersoff potential is used to depict the interaction among the silicon atoms and the interaction between diamond atoms and silicon atoms. The cutting speed used in this paper is between 25 and 200 m/s.

2.2 Characterization of tool edges

To investigate the influence of asymmetric tool edge shape on cutting performance, parameters should be determined to characterize the cutting edge shape. The form factor method proposed by Denkena et al. [23] has been applied to investigate the cutting performance of the cutting tool. However, too many parameters may inhibit its applications in practice. In 2012, Denkena et al. [30] proposed a parameter which is called as a normalized ploughing zone, and its influence on the tool wear, burr formation, and residual stress has been investigated. In this paper, the tool edge radius is still used and modified to characterize the tool edge shape. According to the former study, the feed forces and the ploughing force in the feed direction which is separated from the total process force are more sensitive to a change in the cutting edge radius than forces in the cutting direction [12, 20]. When the cutting tool edge is characterized by the form factor method mentioned, the process forces are mostly affected by the edge segment on the flank face, S_α, whereas the impact of the segment on the rake face, S_γ, is negligible [10]. Except for the process force, the surface integrity is also influenced by the tool edge especially the shape under the stagnation point [30]. Therefore, the cutting edge profile especially the part close to the flank face influences the cutting process more than the edge profile in the rake face side. The tool edge radius fitted to characterize the tool edges should more represent the profile of the edge in the flank face side.

In the former method, the edge radius r_w is fitted using the whole profile of the cutting edge. For characterizing the tool edge performance more precisely, profile data in the rake face side could not participate the edge radius fitting process. A modified tool edge radius r_β fitted only using the profile in the flank face side, line SG in Fig. 3, is proposed to describe the geometry of the cutting tool edge. The stagnation point S shown in Fig. 3 is thought to be a cut-off point separating the edge profile into two parts: profile in the flank face and rake face side. The position of the stagnation point is determined by an effective rake angle at the tool edge profile [19]. According to the analysis in the next section, it is at a range of −42.0° to −50.7° for three different cutting edges. The fitted tool edge radius r_β shown in Table 1 is calculated with the effective rake angle at an average value of −46°. For cutting edge T1, the fitted tool edge radius r_β is slight smaller than that of T2. The r_β of T3 is two times larger than that of T2. If the radius of T1 and T3 is fitted with the whole profile, the value of r_w is equal to each other. Therefore, the difference of the asymmetric tool edge could be distinguished by using the parameter r_β. Comparing to the method proposed by Denkena et al., the tool edge is still characterized by the edge radius r_β. If taking the profile in the flank face side as a circle, the normalized ploughing zone is in linear relationship with the tool edge radius r_β. The ploughing zone is linear with the

Table 1 Parameters in reconstruction of the tool edges

Tool edge no.	$\alpha = 8°, \gamma = 0°$							
	K	S_α (nm)	S_γ (nm)	Δr (nm)	φ (°)	r_s (nm)	r_w (nm)	r_β (nm)
1	*2*	5.75	11.50	2.64	*−6.2*	5	8.30	3.54
2	*1*	5.75	5.75	2.62	*0*	5	5.01	4.99
3	*0.5*	11.50	5.75	2.64	*6.2*	5	8.30	11.06

square of the tool edge radius r_β^2. Detailed tool edge information is shown in Table 1, and the results show that the fitted tool edge radius r_β increases with the decrease of form factor K. In next the section, the influences of the tool edge radius r_β on the stagnation region, subsurface damage, and cutting force are discussed.

3 Results and discussion

3.1 Stagnation region

Figure 4 is snapshots of the MD simulations when the cutting distance is 30 and 10 nm and the cutting tool edge is T3. To investigate the evolution of the stagnation region in a cutting process, atoms which tend to form a chip and a machined surface are respectively assigned with blue and green colors. Atoms in front of the tool rake face and above the workpiece surface are thought to form a chip, and the atoms beneath the tool flank face are thought to form a machined surface, as shown in Fig. 4a. Then, the atom motion in the cutting process and the boundary of the atoms tend to form a chip, and the machined surface could be observed when the MD simulation results were replayed. In Fig. 4b which is the snapshot with the cutting distance of 10 nm, a small red triangular region could be obviously seen in front of the cutting tool edge and more atoms would join in and maintain the region with the cutting process. A displace vector of atoms in front of the tool edge is shown in Fig. 7a. The displacement vector of stagnated red atoms in the region is equal to zero which means the entrapment by the cutting edge do not form a chip and machined surface, or they should take more time and cutting distance to determine whether to be a part of a chip or machined surface. This region is recognized as the stagnation region in the cutting process. Atoms above the stagnation region tend to form a chip, and atoms below the stagnation region are ploughing to form a machined surface. Between the blue and green atoms, there is a layer of red atoms which could be seen as a separation layer. Atoms in this layer tend to participate the evolution of the stagnation region. In order to obviously observe the evolution of atoms in this layer, the atoms is separated into three parts, assigned with black, yellow, and violet colors respectively, and marked from A1 to A3 as shown in Fig. 5a. As the tool cutting into the workpiece, the atoms in the region A1 colored by black are quickly adhere around the tool edge. After that, the yellow atoms in the region A2 are converged in the stagnation region, as shown in Fig. 5b. The converged yellow atoms are then pressured and tend to spread along the tool edge. The violet atoms marked as A3 would experience the same evolution as the yellow atoms have with a further cutting process, as shown in Fig. 5c. Finally, the yellow and violet atoms flow around the tool edge to form a chip or machined surface. Unlikely to the yellow and violet atoms, it would take longer time or cutting distance for the black atoms to get rid of the adhesive force from the tool edge. The black atoms would just adhere around the tool edge, as shown in Fig. 5b–d, to form a membrane of workpiece atoms.

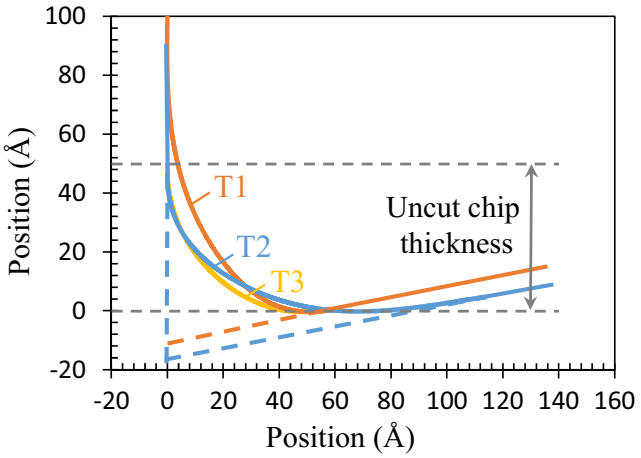

Fig. 2 Reconstructed cutting tool edge

According to Fig. 5, the stagnation region tends to form at the beginning of a cutting process. Then, the size of the stagnation region increases with the cutting distance until it becomes stable. The number of atoms in the stagnation region which represents the size of the stagnation region is calculated with the cutting distance changing from 5 to 20 nm and cutting speed at a range of 25 to 200 m/s for three cutting edges T1, T2, and T3, as shown in Fig. 6a–c. The results reveal that the stagnation region is enlarged with an increase of the cutting distance and the stable state is not attained due to the cutting distance in this paper, which is relatively small. For the cutting edge T1, the size of the stagnation region decreases with the simulated cutting speed change from 25 to 200 m/s except for an obvious increases at cutting speed of 150 m/s and a slight

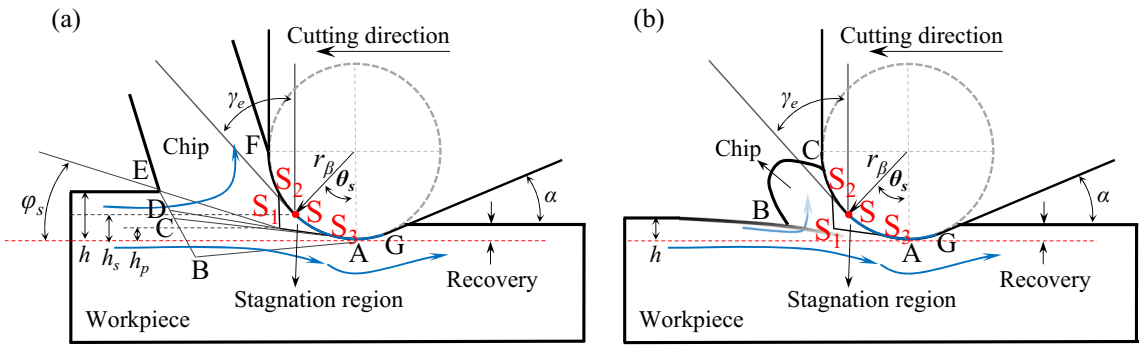

Fig. 3 Nano-cutting model with UCT. **a** Larger than h_{min}. **b** Similar or less than h_{min}

increase at 50 m/s. For T2, the stagnation region size decreases with the cutting speed changing from 10 to 100 m/s. When further increasing the cutting speed, fluctuation happens (attain peak at the cutting speed of 150 m/s and valley at the cutting speed of 175 m/s). For the cutting edge T3, the size of the stagnation region decreases with the simulated cutting speed change from 25 to 200 m/s. Two slight increases and an obvious increase could be seen at the cutting speed of 75, 200, and 150 m/s. The stagnation region of the cutting edge T3 at the cutting distance of 17 nm with the cutting velocity of 25 and 100 m/s is shown in Fig. 7; the difference of size could be obviously observed. Generally, the stagnation region size of T2 is smaller than that of T1 and T3. For the cutting speed of 150 m/s, the stagnation region shows an increase for all the cutting edges. And the stagnation region is almost the smallest at the cutting speed of 100 m/s.

For precisely characterizing location of the stagnation region, a cutting model is proposed as shown in Fig. 3. The triangular zones S_1, S_2, and S_3 are the stagnation region, where S_1 is the tip of the stagnation region. It determines the separation of materials in front of the cutting edge. Its vertical distance to the bottom of the cutting edge could be seen as material ploughing thickness h_p. Lines S_1D and S_3C determine the separation layer where the atoms tend to participate the evolution of the stagnation region. Its average height related to the bottom of the cutting edge is marked as h_s which indicates the separation boundary in a subsurface of workpiece material before the cutting process. The separation height h_s is larger than the material ploughing thickness h_p due to the materials in front of the tool edge, which are pressed down. The intersection point of the separation layer with the tool edge profile is defined as the stagnation point S which has also been defined by Lai et al. [17].

Two stagnation region characterization parameters (material ploughing thickness h_p and separation height h_s) of three tool edges in different cutting speeds are shown in Fig. 8. The relation $h_p < h_s$ could be obviously observed. For all the three cutting edges, two parameters all slightly decrease with the cutting speed, except for the cutting edge T1, whose parameter values increase at the cutting speed of 75 m/s and its ploughing thickness h_s shows a decrease at the cutting speed of 125 m/s. In further MD analysis, it is found that the material minimum UCT $h_{\min}$ is equal to the separation height h_s. Therefore, h_s becomes an important parameter to determine the minimum UCT for tool edges with different tool edge shapes. As shown in Fig. 8c, minimum UCT for T3 is larger than that for T1 and T2. The minimum UCT of T1 is slight smaller than that of T2. The corresponding effective rake angles γ_e for minimum UCT of T1, T2, and T3 are −41.98°~−47.4°, −45.4°~−49.9°, and −47°~−50.7°, respectively. The results show that the large newly proposed tool edge radius r_β would cause an increase of minimum UCT.

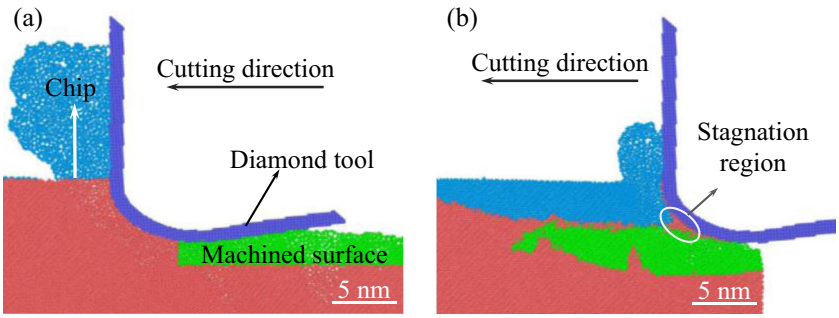

Fig. 4 Snapshots of the MD simulations with the cutting distance of **a** 30 and **b** 10 nm

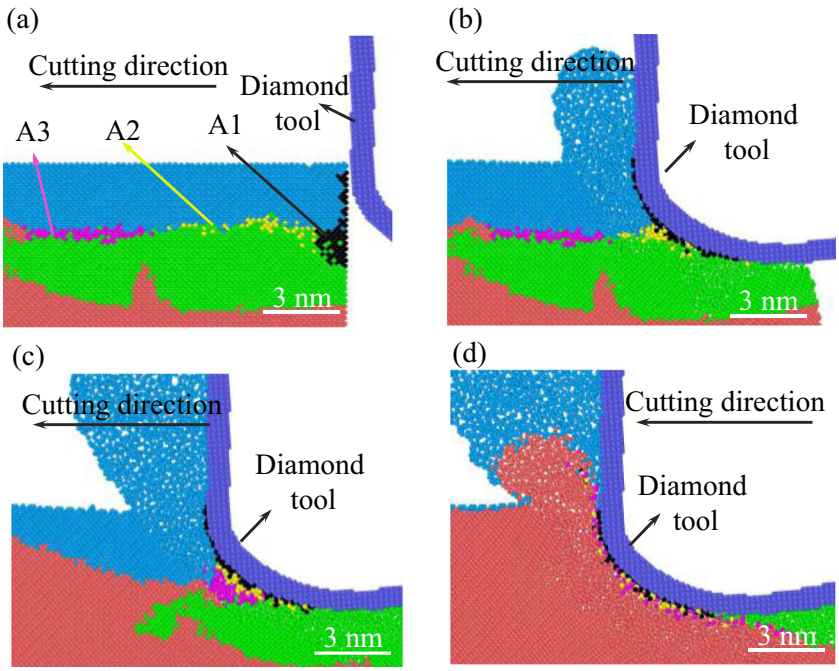

Fig. 5 Evolution of the stagnation region

3.2 Chip formation

When the UCT is larger than the minimum UCT, a shear line is assumed to start at the stagnation point [31]. However, with the MD results shown in Fig. 7, the shear line starts at the tip of the stagnation region. Therefore, a modified cutting model with the UCT larger than minimum UCT is shown in Fig. 3 with the shear line start at the stagnation region tip S_1 and marked as S_1E. In this condition, the stagnation region could be seen as a new formed tool edge to participate the cutting process making the material removed in the shearing process. In order to observe the chip formation, the atoms of silicon have been layered with different colors. The angle between the layers and the cutting direction is approximately equal to the shear angle φ_s, which is 40°~42° for tool T1 and T2 and 34°~35° for tool T3. With the cutting process, more atoms are sheared to form chips, and due to the strong interaction force between silicon and diamond atoms, the chip tends to curl clockwise. Detailed information of chip formations is shown in Fig. 9. This kind of the material removal mechanism is different from the former proposed extrusion mechanism [32], due to the UCT used which is almost equal to the basic radius r_s. In Fig. 9b, the tool edge T2 displays a different phenomenon that workpiece atoms tend to gather around the stagnation point and enlarge the area of the stagnation region.

When the UCT is similar to or smaller than h_{min}, the stagnation region also exists and the composed atoms are mainly

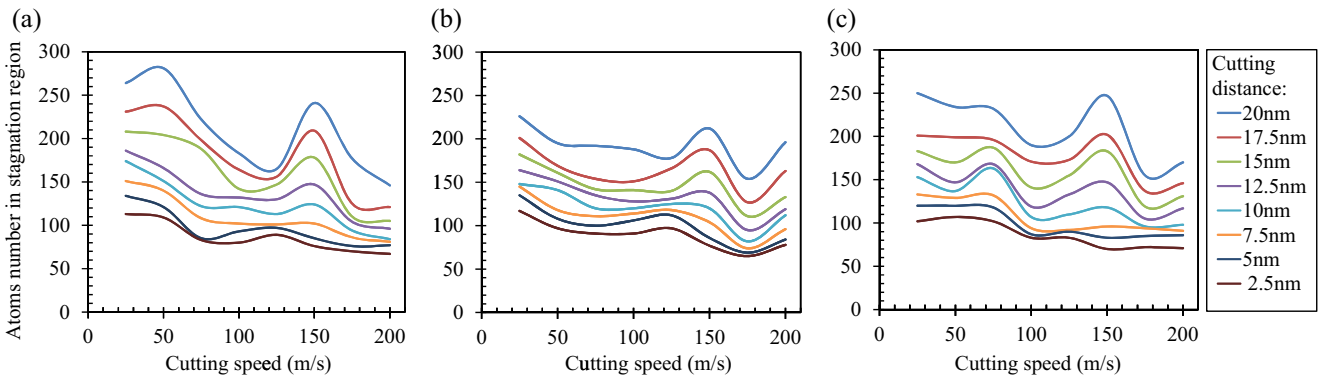

Fig. 6 Number of atoms in the stagnation region for **a** T1, **b** T2, and **c** T3

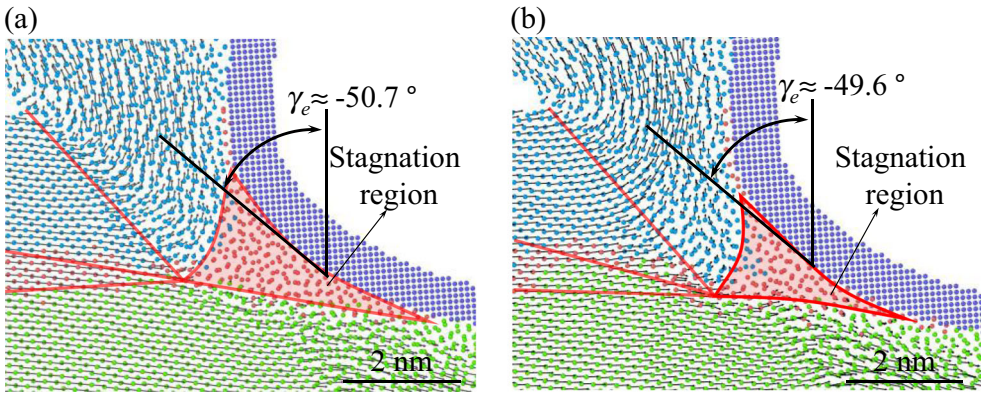

Fig. 7 The stagnation region at the cutting distance of 17 nm with the cutting velocity of **a** 25 and **b** 100 m/s for T3

in the initial cutting region colored with red as shown in Fig. 10a, b. The initially stagnated atoms are trapped and moving following the cutting edge. In the first 10-nm cutting distance, atoms in the upper layer of workpiece assigned with blue color, as shown in Fig. 10a tend to be extruded forming the initial chip. After that, the atoms in the upper layer separate into three kinds: forming as a chip (blue color), machined subsurface (green color), and stagnated atoms (red color), as shown in Fig. 10b. Therefore, the chip grows slowly with the cutting process, and large parts of atoms are ploughed under the action of the cutting edge. When the UCT is larger than $h_{\min}$, the stagnation region, in some extent, could be seen as a new formed tool edge to participate the cutting process, as shown in Fig. 7. However, when it is smaller than or similar to $h_{\min}$, the stagnation region is not tough enough to cut the materials making it to slide on the surface. As shown in Fig. 10c which is the displacement of the atoms in the Y direction, there is an obvious boundary which indicates the pressed workpiece surface. The displacement vector is shown in Fig. 10d which also illustrates the sliding process. An extrusion model in nano-cutting process is shown in Fig. 3b. During the sliding process, a part of the atoms of the upper layer of a workpiece surface is extruded to form the chip. The atom is removed in extrusion mechanism which is different from the shearing mechanism, when the UCT is similar or less than the minimum UCT.

3.3 Subsurface damage

As shown in Fig. 11d, the chip is colored with dark green and the subsurface of the machined surface is layered by different colors in order to observe the evolution of atoms obviously. Three peak-like atom distributions could be seen and marked as D1, D2, and D3. It means that the atoms in the peak-like region would be pinned into the material with the cutting process. In Fig. 11b, the D2 region is pressed by the cluster mainly composed of green atoms and the D3 region is pressed by the violet and blue atom-composed cluster, as shown in Fig. 11c. After the tool cutting over the peak-like regions, the atoms in the regions are completely pinned into the materials, causing the subsurface damages, as shown in Fig. 12c. The damaged subsurface also composes of several peak-like regions which is inverted, and the position of the peaks is in coincidence with the peaks in Fig. 11a. The peak-like region D1 is smaller than the D2 and D3, therefore causing a smaller subsurface damage region. The material phase of the damaged layer has transformed from a single-crystal phase to amorphous phase. The green atoms surrounded by the violet atoms form the upper layer of the machined surface, and almost all of them are transformed from a single-crystal phase to amorphous phase. The upper and left side violet atoms are almost phase-transformed to the amorphous phase. But only a part of the violet atoms under the green atoms transformed to the

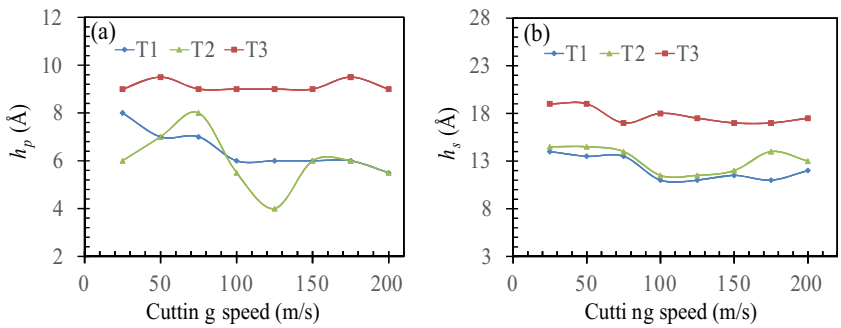

Fig. 8 **a** Material ploughing thickness h_p and **b** separation height h_s

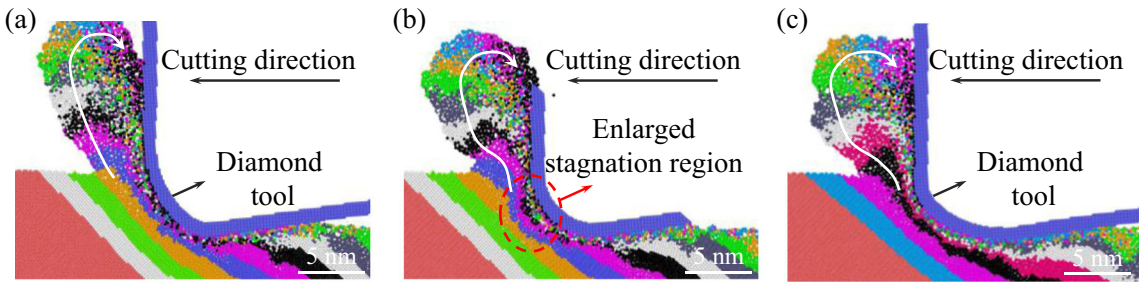

Fig. 9 Chip formation for **a** T1, **b** T2, and **c** T3 with UCT of 5 nm

amorphous phase due to the atoms in the peak-like region. These phenomena are also found in cutting of silicon with T1 and T2 cutting edges as shown in Fig. 12a, b.

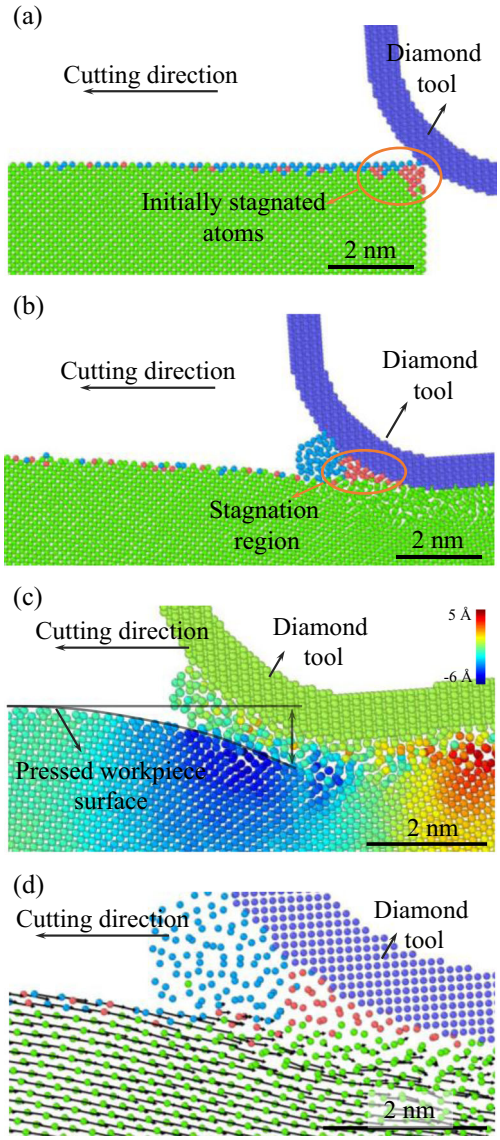

Fig. 10 The cutting process under UCT similar to h_{min} for T2 with the cutting distance of **a** 0 and **b** 20 nm and **c** displacement in Y direction and **d** displacement vector

The depth of the damaged layer and the percentage of phase-transformed atoms in the machined subsurface with cutting speed change from 25 to 200 m/s for the tool edges T1, T2, and T3 are calculated, and the results are shown in Fig. 13. Due to the part of the phase-transformed material underneath the tool edge which would recover to single-crystal silicon, the damage depth is obtained when the cutting tool edge cutting over and the flank face has departed from the machined surface. Results show that the depth of a damaged layer for the cutting edge T3 is larger than that for T2. The damaged depth of T2 is larger than that of T1 except at the cutting speed of 125 m/s. The atoms in the damaged layer have also been counted and find that the cutting edge T3 causes the largest phase transformation in three cutting edges. The phase-transformed atoms when cutting using T2 are similar to that of T1 but fluctuate with the value of T1. The results reveal that the subsurface damage, both the depth of damaged layer and the percentage of phase-transformed atoms, is aggravated with the increase of the newly proposed tool edge radius r_β.

3.4 Cutting force

The process forces in the cutting and feed direction have been derived from the interaction between the tool and workpiece atoms. At the beginning of the cutting process, the force in the cutting and feed direction increases with the cutting time and attains the stable state when the cutting distance is about 10 nm. The average cutting force and feed force are calculated within the cutting distance at the range of 10~35 nm. The results are shown in Fig. 14. The average cutting forces for tool edges T1, T2, and T3 are almost the same which reveals that the tool edge shape has less influence on the process force in the cutting direction. The average feed force for tool T3 is larger than that of T2 and T3. It is in coincident of the newly proposed tool radius r_β which would cause a larger feed force with its increase. When the cutting speed is less than 100 m/s, the feed force of T1 is slight larger than that of T2. But when the cutting speed is beyond 100 m/s, the feed force of T1 is smaller than that of T2. This is because the discrepancy of T1 and T2 is small which would not cause an obvious difference

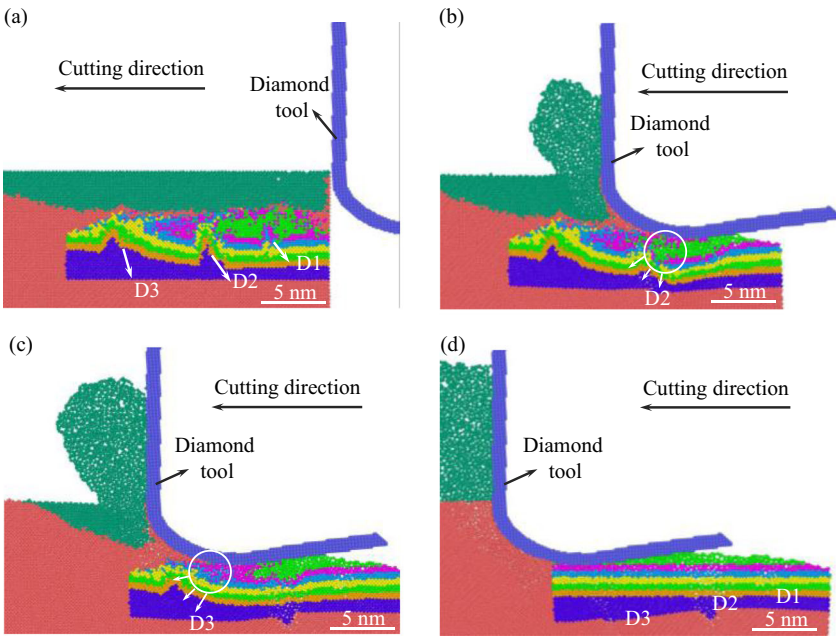

Fig. 11 Atom motion in the silicon subsurface with different cutting distances

in feed force. Therefore, the former used tool edge radius r_w could not characterize the magnitude of process force precisely, especially the force in feed direction, when the tool edge used is asymmetric. In this condition, the newly proposed radius r_β could be used to determine the magnitude of feed force and the ratio of average cutting force to feed force, which actually determines the direction of resultant force acting on the tool edge.

4 Conclusions

Tool edges with different forms have been reconstructed, and a parameter r_β different from the former used tool edge radius r_w has been proposed to characterize the tool edge especially when it is asymmetric. The influences of the asymmetric tool edges on the stagnation region, chip formation, subsurface damage, and cutting forces have been investigated by using MD simulation. The conclusions can be drawn as follows:

1. The stagnation region in front of the tool edge has been confirmed, and its size increases with the cutting distance and decreases with an increase of the cutting speed. The location of the stagnation region has been characterized by the material ploughing thickness h_p and separation height h_s. The separation height h_s also determines the minimum UCT and the stagnation point. The minimum UCT tends to increase with the newly proposed tool edge radius r_β. The corresponding effective rake angle for three reconstructed tools is at the range of −42° to −51°, and the absolute value becomes larger with an increase of the newly proposed tool edge radius r_β.
2. When the UCT is larger than minimum UCT, the stagnation region formed in the cutting process could be seen as a newly formed cutting edge to participate the cutting process, making the material removed in shearing mechanism and the shearing line starting at the tip of stagnation region. The shear angle for the tool with small r_β is smaller than that for the tool with large r_β. When the UCT is

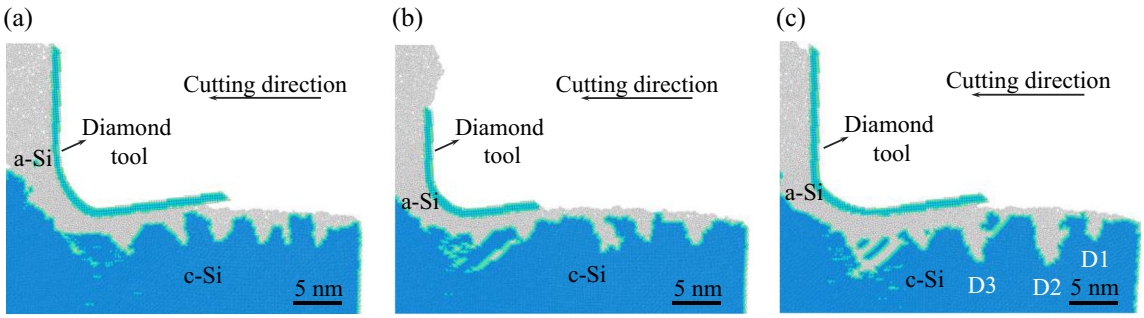

Fig. 12 Subsurface damage at the cutting speed of 200 m/s for **a** T1, **b** T2, and **c** T3

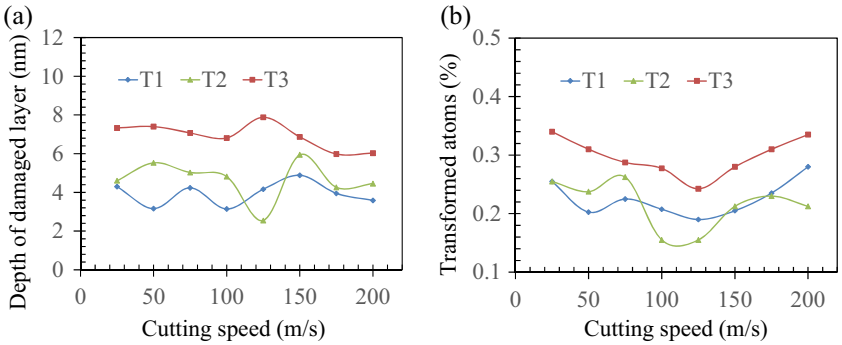

Fig. 13 Subsurface damage. **a** Depth of a damaged layer. **b** Phase-transformed atoms

similar or smaller than minimum UCT, the stagnation region is not tough enough to cut the materials making it slide on the surface. During the sliding process, a part of the atoms of the upper layer of a workpiece surface is removed by extrusion. Two models have been proposed to describe the shearing and extrusion mechanism in the nano-cutting process.

3. In the nano-cutting process, atoms in the workpiece subsurface form several peak-like regions that would be pinned into the material causing an inverted peak-like subsurface damage. The subsurface damage, both the damage depth and the percentage of the phase-transformed atoms, is aggravated with an increase in the newly proposed tool edge radius r_β.
4. The cutting force in feed direction increases with the newly proposed tool edge radius r_β, which the former used tool edge radius r_w could not characterized precisely, especially when the tool edges are asymmetric.
5. Combined with the former used tool edge radius r_w, the proposed tool edge parameter r_β which is the fitted tool edge radius with the edge profile at the flank face side could be used to characterize the cutting performance of a cutting tool and reduce discrepancies in describing the tool edge, especially when it is asymmetric.

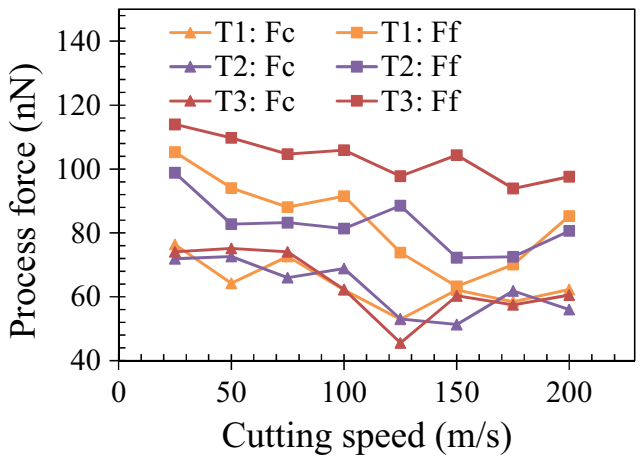

Fig. 14 Cutting force for the cutting edges T1, T2, and T3

Acknowledgements The authors thank the supports of the National Natural Science Foundation (Grant No. 51320105009 & 91423101) and the "111" project by the State Administration of Foreign Experts Affairs and the Ministry of Education of China (Grant No. B07014).

References

1. Merchant ME (1945) Mechanics of the metal cutting process. I. Orthogonal cutting and a type 2 chip. J Appl Phys 16(5):267–275
2. Merchant ME (1945) Mechanics of the metal cutting process. II. Plasticity conditions in orthogonal cutting. J Appl Phys 16(6):318–324
3. Weule H, Hüntrup V, Tritschler H (2001) Micro-cutting of steel to meet new requirements in miniaturization. CIRP Ann 50(1):61–64
4. Özel T (2009) Computational modelling of 3D turning: influence of edge micro-geometry on forces, stresses, friction and tool wear in PcBN tooling. J Mater Process Technol 209(11):5167–5177
5. Denkena B, Lucas A, Bassett E (2011) Effects of the cutting edge microgeometry on tool wear and its thermo-mechanical load. CIRP Ann 60(1):73–76
6. Özel T, Karpat Y, Srivastava A (2008) Hard turning with variable micro-geometry PcBN tools. CIRP Ann 57(1):73–76
7. Woon KS, Rahman M (2010) The effect of tool edge radius on the chip formation behavior of tool-based micromachining. Int J Adv Manuf Technol 50(9–12):961–977
8. Wu X, Li L, Zhao M, He N (2015) Experimental investigation of specific cutting energy and surface quality based on negative effective rake angle in micro turning. Int J Adv Manuf Technol 82(9):1941–1947
9. Liu ZQ, Shi ZY, Wan Y (2013) Definition and determination of the minimum uncut chip thickness of microcutting. Int J Adv Manuf Technol 69(5–8):1219–1232
10. Denkena B, Biermann D (2014) Cutting edge geometries. CIRP Ann 63(2):631–653
11. Chien KL (1953) The influence of tool sharpness on the mechanics of metal cutting (PhD) Massachusetts Instiute of Techn Cambridge
12. Albrecht P (1960) New developments in the theory of the metal-cutting process: part I. The ploughing process in metal cutting. J Eng Ind 82(4):348–357
13. Fang FZ, Venkatesh VC (1998) Diamond cutting of silicon with nanometric finish. CIRP Ann 47(1):45–49
14. Kim CJ, Bono M, Ni J (2002) Experimental analysis of chip formation in micro-milling technical papers—SME
15. Ikawa N, Shimada S, Tanaka H (1992) Minimum thickness of cut in micromachining. Nanotechnology 3(1):6
16. Karpat Y, Özel T (2008) Mechanics of high speed cutting with curvilinear edge tools. Int J Mach Tools Manuf 48(2):195–208

17. Lai M, Zhang XD, Fang FZ (2012) Study on critical rake angle in nanometric cutting. Appl Phys A Mater Sci Process 108(4):809–818
18. Kountanya RK, Endres WJ (2001) A high-magnification experimental study of orthogonal cutting with edge-honed tools. In: Proceedings of 2001 ASME International Mechanical Engineering Congress and Exposition, New York
19. Fang FZ, Zhang GX (2003) An experimental study of edge radius effect on cutting single crystal silicon. Int J Adv Manuf Technol 22(9):703–707
20. Wyen CF, Wegener K (2010) Influence of cutting edge radius on cutting forces in machining titanium. CIRP Ann 59(1):93–96
21. Wyen CF, Knapp W, Wegener K (2011) A new method for the characterisation of rounded cutting edges. Int J Adv Manuf Technol 59(9):899–914
22. Yussefian NZ, Koshy P (2013) Parametric characterization of the geometry of honed cutting edges. Precis Eng 37(3):746–752
23. Denkena B, Reichstein M, Brodehl J, de León García L (2005) Surface preparation, coating and wear performance of geometrically defined cutting edges. In: Proceedings of the 5th international conference the coatings in manufacturing engineering. pp 5–7
24. Zong WJ, Li D, Sun T, Cheng K (2006) Contact accuracy and orientations affecting the lapped tool sharpness of diamond cutting tools by mechanical lapping. Diam Relat Mater 15(9):1424–1433
25. Moriwaki T (1989) Machinability of copper in ultra-precision micro diamond cutting. CIRP Ann 38(1):115–118
26. Li XP, Rahman M, Liu K, Neo KS, Chan CC (2003) Nano-precision measurement of diamond tool edge radius for wafer fabrication. J Mater Process Technol 140(1–3):358–362
27. Gao W, Motoki T, Kiyono S (2006) Nanometer edge profile measurement of diamond cutting tools by atomic force microscope with optical alignment sensor. Precis Eng 30(4):396–405
28. Gao W, Asai T, Arai Y (2009) Precision and fast measurement of 3D cutting edge profiles of single point diamond micro-tools. CIRP Ann 58(1):451–454
29. Bassett E, Köhler J, Denkena B (2012) On the honed cutting edge and its side effects during orthogonal turning operations of AISI1045 with coated WC-Co inserts. CIRP J Manufact Sci Tech 5(2):108–126
30. Denkena B, Koehler J, Rehe M (2012) Influence of the honed cutting edge on tool wear and surface integrity in slot milling of 42CrMo4 steel. Procedia CIRP 1:190–195
31. Fang FZ, FF X, Lai M (2015) Size effect in material removal by cutting at nano scale. Int J Adv Manuf Technol 80(1–4):591–598
32. Fang FZ, Wu H, Liu YC (2005) Modelling and experimental investigation on nanometric cutting of monocrystalline silicon. Int J Mach Tools Manuf 45(15):1681–1686